Two Temporal Phases of Light Adaptation in Retinal Rods

Peter D. Calvert,[1] Victor I. Govardovskii,[2] Vadim Y. Arshavsky,[1] and Clint L. Makino[1]

[1]Department of Ophthalmology, Harvard Medical School, Massachusetts Eye and Ear Infirmary, Boston, MA 02114
[2]Institute of Evolutionary Physiology and Biochemistry, Russian Academy of Science, 194223 St. Petersburg, Russia

ABSTRACT Vertebrate rod photoreceptors adjust their sensitivity as they adapt during exposure to steady light. Light adaptation prevents the rod from saturating and significantly extends its dynamic range. We examined the time course of the onset of light adaptation in bullfrog rods and compared it with the projected onset of feedback reactions thought to underlie light adaptation on the molecular level. We found that adaptation developed in two distinct temporal phases: (1) a fast phase that operated within seconds after the onset of illumination, which is consistent with most previous reports of a 1–2-s time constant for the onset of adaptation; and (2) a slow phase that engaged over tens of seconds of continuous illumination. The fast phase desensitized the rods as much as 80-fold, and was observed at every light intensity tested. The slow phase was observed only at light intensities that suppressed more than half of the dark current. It provided an additional sensitivity loss of up to 40-fold before the rod saturated. Thus, rods achieved a total degree of adaptation of ~3,000-fold. Although the fast adaptation is likely to originate from the well characterized Ca^{2+}-dependent feedback mechanisms regulating the activities of several phototransduction cascade components, the molecular mechanism underlying slow adaptation is unclear. We tested the hypothesis that the slow adaptation phase is mediated by cGMP dissociation from noncatalytic binding sites on the cGMP phosphodiesterase, which has been shown to reduce the lifetime of activated phosphodiesterase in vitro. Although cGMP dissociated from the noncatalytic binding sites in intact rods with kinetics approximating that for the slow adaptation phase, this hypothesis was ruled out because the intensity of light required for cGMP dissociation far exceeded that required to evoke the slow phase. Other possible mechanisms are discussed.

KEY WORDS: photoreceptors • phototransduction • adaptation • calcium • cGMP

INTRODUCTION

Vertebrate retinal rod photoreceptors respond to changes in light intensity over an enormous range of ambient light levels. Rods are able to signal the absorption of single photons by their photopigment rhodopsin, yet remain responsive to changes in intensity when the ambient illumination activates 10^3–10^4 rhodopsins/s. This ability is achieved by a delicate balance between mechanisms that provide a high signal amplification in the phototransduction cascade and adaptive mechanisms that prevent response saturation (for reviews see Bownds and Arshavsky, 1995; Pugh et al., 1999; Pugh and Lamb, 2000; Burns and Baylor, 2001; Fain et al., 2001).

After a molecule of rhodopsin in the photoreceptor outer segment absorbs a photon, it serially activates G proteins (transducins) in the first amplifying stage in phototransduction. Each activated transducin (T*) stimulates the activity of a single catalytic subunit of cGMP phosphodiesterase (PDE*), which hydrolyzes cytoplasmic cGMP in a second stage of amplification. In frog rods, a single molecule of photoactivated rhodopsin (R*) produces ~150 T* s^{-1} and each PDE* hydrolyzes several hundred molecules of cGMP s^{-1} (Leskov et al., 2000). Highly cooperative control of cGMP-gated channels on the plasma membrane of the rod outer segment (ROS)* provides a further 2- to threefold amplification. The reduction in cGMP causes the closure of these channels interrupting the inward flow of Na^+ and Ca^{2+}. The resultant reduction in inward current constitutes the photoresponse. At the peak of the single photon response, which in frogs occurs in ~1 s after photon absorption, ~5% of the open, light-sensitive channels become closed. So, if the photoreceptor simply summed the effects of each photon captured, then steady illumination providing <100 R* s^{-1} would close all of the light-sensitive channels, rendering the rod blind to further increases in light intensity. Light adaptation efficiently prevents response saturation, thus, preserving differential light sensitivity and vastly extending the operative range of the rod.

Light adaptation is thought to be mediated by an array of feedback mechanisms that respond to the light-dependent Ca^{2+} decline in the ROS. These mechanisms modulate the activities and/or catalytic lifetimes of individual components of the phototransduction system. Two mechanisms extend the operating range of the rod in steady light by opposing the effect of light-activated cGMP hydrolysis. First, Ca^{2+} decline increases the rate of cGMP synthesis by guanylate cyclase, coun-

Address correspondence to Peter D. Calvert, Ph.D., Department of Ophthalmology, Harvard Medical School, Massachusetts Eye and Ear Infirmary, 243 Charles Street, Boston, MA 02114. Fax: (617) 573-4290; E-mail: pdcalvert@meei.harvard.edu

*Abbreviation used in this paper: ROS, rod outer segment.

tering cGMP exhaustion by PDE* (Koch and Stryer, 1988). This effect is mediated by guanylate cyclase–activating proteins (Palczewski et al., 1994; Dizhoor et al., 1995). Second, the affinity of the light-sensitive channels for cGMP increases in low Ca^{2+} through a mechanism mediated by Ca^{2+}-calmodulin or a related protein (Hsu and Molday, 1993; Gordon et al., 1995; Nakatani et al., 1995; Sagoo and Lagnado, 1996), allowing the channels to open at lower cGMP concentrations than in the dark-adapted rod. Another Ca^{2+} feedback mechanism accelerates the rate of R* phosphorylation by rhodopsin kinase (Kawamura, 1993; Chen et al., 1995; Klenchin et al., 1995). This mechanism, mediated by the Ca^{2+}-binding protein recoverin (also called S-modulin in frogs), causes R* to signal for a shorter time and thereby reduces the total amount of cGMP hydrolyzed after absorption of each photon.

Light adaptation may also involve calcium-independent feedback mechanisms. cGMP dissociation from noncatalytic binding sites located on the PDE molecule accelerates the rate of transducin GTPase activity, cutting short the lifetime of the T–PDE* complex (Arshavsky et al., 1991; Arshavsky and Bownds, 1992; Calvert et al., 1998). It was hypothesized that in steady light, the sustained hydrolysis of cGMP in rods would lead to cGMP dissociation from the noncatalytic sites, accelerating the shutoff of T–PDE*, thus, reducing the number of cGMP molecules hydrolyzed by each PDE.

Previous studies indicated that some aspects of light adaptation are established very quickly after the onset of light (Matthews, 1996; Murnick and Lamb, 1996), whereas other aspects are observed only after prolonged exposure (Dowling and Ripps, 1972; Coles and Yamane, 1975; Fain, 1976; Cervetto et al., 1981; Forti et al., 1989). Our goal was to systematically analyze the time course and light intensity dependence of light adaptation in frog rods. We show that adaptation to prolonged continuous illumination occurs in two distinct temporal phases: one engages in seconds after the onset of light, and another requires tens of seconds to fully operate. The fast phase is present at all intensities and lowers rod light sensitivity by ~80-fold. The slow phase operates only at light intensities sufficient to suppress over 50% of the rod's dark circulating current and contributes an additional >40-fold reduction in sensitivity.

MATERIALS AND METHODS

Animals and Tissue Preparation

All experiments were conducted in accordance with the National Institutes of Health *Guide for the Care and Use of Laboratory Animals.* Adult bullfrogs (*Rana catesbeiana*) were purchased from Charles Sullivan and were maintained under a 12-h flickering light/12-h dark cycle. A shallow pool of charcoal-filtered tap water (19–22°C) was continuously turned over in their pens. Frogs were hand-fed puréed dog food (Purina) supplemented with AIN-76A fat soluble vitamin mix (Research Diets, Inc.). Before an experiment, animals were dark-adapted for at least 12 h. All subsequent tissue manipulations were performed under infrared illumination. Animals were anesthetized by cooling in an ice bath, decapitated, and their spinal cords and brains were pithed. Eyes were enucleated, and the retinas were isolated in Ringer's solution. Retinal tissue was stored on ice for up to 48 h.

Solutions

Ringer's-bicarbonate solution contained the following (in mM): 98 NaCl, 2.5 KCl, 1.0 $MgCl_2$, 10 HEPES (monosodium salt), 1.5 $CaCl_2$, 0.02 EDTA, 10 $NaHCO_3$, and 10 glucose, pH 7.5. Osmolarity was adjusted to 230 mOsm by the addition of 10× Ringer's-bicarbonate or H_2O. Bicarbonate, which is known to affect the phototransduction machinery (Baylor et al., 1984; Meyertholen et al., 1986; Donner et al., 1990), was included to more closely reproduce physiological conditions (Hare and Owen, 1998). Electrodes were filled with an identical solution, except that $NaHCO_3$ was replaced with an equivalent concentration of NaCl.

Recording Rod Circulating Current

Photocurrents of single rods were monitored using the suction electrode technique (Baylor et al., 1979a). A small piece of retinal tissue was chopped or shredded and placed into a recording chamber mounted on the stage of an inverted microscope. The entire apparatus was enclosed in a light-tight Faraday cage. The tissue was continuously perfused with Ringer's-bicarbonate equilibrated with 95% O_2 and 5% CO_2 at room temperature (19–22°C). Cells suitable for recording were found by scanning the infrared illuminated chamber with a closed-circuit television system. The outer segment of a rod attached to a small piece of retina was drawn into a suction electrode, and the change in membrane current was recorded with a current-to-voltage converter (Axopatch-200A; Axon Instruments, Inc.). Electrical connections to the bath and the suction pipette were made with agar bridges and calomel half-cells. Recordings were low-pass filtered at 20 Hz (−3 dB, 8-pole Bessel filter; Frequency Devices) and digitized at 200 Hz (Pulse version 7.4; Heka). No corrections were made for the delay introduced by low-pass filtering. Additional digital filtering at 10 Hz was achieved by convolution with a Gaussian. The recordings were also processed with a pulse code modulator (Neuro-corder; Neurodata Instrument Co.) and stored on VHS tape.

Rods were stimulated with a xenon arc lamp (Oriel) whose output was passed through a 500-nm interference filter (10-nm full bandwidth at half-maximal transmission; Omega Optical). A diaphragm in the beam was focused at the level of the cell under infrared illumination. The intensity of the light was adjusted with neutral density filters. The light at 500 nm was calibrated through a 100-μm pinhole (Melles Griot), placed at the level of the recording chamber, using a digital photometer (UDT 350; Graseby Optronics). Light exposure was controlled by an electronic shutter (Uniblitz; Vincent Associates) under the command of a pulse generator (Pulsemaster; World Precision Instruments) and was monitored with a photodiode.

Measurement of cGMP Levels in Intact Frog Rod Outer Segments

Light-dependent changes in the cGMP content of ROS on the intact retina were measured using methods described previously (Govardovskii and Berman, 1981). Briefly, in each experiment, four pieces of bullfrog retina isolated in HEPES-buffered Ringer's were flat-mounted (ROS side out) onto the arms of a computer-controlled, rapid freezing apparatus. One of the four retinal pieces in each experiment remained in darkness as a control. The

other three retinal pieces were exposed to light from a tungsten halogen source. Rods were illuminated axially, so a 580-nm interference filter (10-nm full bandwidth at half-maximal transmission) was imposed in the optical path to achieve uniform photon absorption within the ROS (Makino et al., 1990). At various times after the onset of illumination, the ROSs were brought into contact with a liquid N_2-cooled copper block and frozen within 20–100 ms (Govardovskii and Berman, 1981). ROSs were collected into Eppendorf tubes using a cryomicrotome, 50–150 μl of ice-cold 1 M HCl was added, and the sample was vigorously mixed while the ROS thawed. The total volume of each sample was determined, and the acid-quenched ROSs were centrifuged at 13,000 *g* for 10 min at 5°C. A defined volume of the cGMP-containing supernatant was dried in a Speedvac, redissolved in assay buffer, and the cGMP level was determined using the cGMP scintillation proximity assay (Amersham-Pharmacia). The pellet containing rhodopsin was neutralized with 10 mM Tris, pH 8.8, and dissolved in a solution containing 0.1 M Tris, pH 6.8, and 3% SDS. The amount of rhodopsin in the pellet was determined by a colorimetric DC protein assay (Bio-Rad Laboratories) using purified ROS standards whose rhodopsin content had been determined previously by measuring the difference in absorbance at 500 nm before and after total rhodopsin bleaching (Bownds et al., 1971). Ringer's-bicarbonate was used in several experiments with similar results.

Bullfrog retinas were reported to contain a mixture of pigments (rhodopsin and porphyropsin) particularly in the dorsal field (Reuter et al., 1971). The pigments differ in the identity of their chromophore: rhodopsin consists of opsin bound to 11-cis retinal, whereas porphyropsin consists of the same opsin bound to 3,4-dehydro, 11-cis retinal. Since the two pigments have different spectral properties, it was necessary to characterize the pigment contents of our frog rods to properly calculate the rate of bleaching by the 580-nm light. We did not detect porphyropsin in the total retinal pigment extract from the frogs used in this study, as determined by applying a pigment absorbance template (Govardovskii et al., 2000) to difference spectra, although the sensitivity of the method could not rule out a quantity of porphyropsin <5%. During visual inspection of the frozen retinal fragments any small patches of different coloration that could contain porphyropsin were removed before cryodissection of the ROS.

For comparison to physiological experiments, the light source was calibrated using a photometer (Graseby Optronics). The bleaching rate was also measured experimentally. Pieces of retina were mounted on the freezing arm, and either were kept in darkness or illuminated with unattenuated, 580-nm light for up to 1,000 s before freezing. Retinal pieces were then thawed in Ringer's solution in darkness, and ROSs were crudely isolated from the rest of the retina by brief vortexing followed by sedimentation of the retinal fragments. Bleaching was determined by difference spectrophotometry before and after regeneration of the sample with 11-cis retinal. The effective light intensities determined from the two methods differed by <10%.

RESULTS

The Magnitude and Onset Kinetics of Light Adaptation

Upon exposure to continuous illumination of moderate intensity, the rod photoresponse rises to a peak and then partially recovers due to a reduction in the rod sensitivity to light, a characteristic of light adaptation (Baylor et al., 1979b). Fig. 1 A shows an example of this behavior. At intensities that approached rod saturation, the partial recovery of the response exhibited at least two phases. There was a fast sag that brought the rod away from saturation, followed by a slower sag that developed over tens of seconds of illumination. With much higher intensities, the fast sag was no longer observed. But after a delay of several tens of seconds, the slow sag still provided some relief from saturation. The presence of two temporally distinct phases of light adaptation is not unique to the bullfrog. Evidence for their existence can be seen in rods of toad (Fain, 1976; Baylor et al., 1980), salamander (Matthews, 1990), skate (Dowling and Ripps, 1972), and newt (Forti et al., 1989).

To characterize adaptation quantitatively, we define sensitivity as a parameter that is inversely proportional to the light intensity necessary to produce a certain fixed level of photoresponse. Note that the decrease in sensitivity to steady light is accompanied by an increase in differential sensitivity, which is essentially the goal of light adaptation. However, we shall restrict our use of the term "sensitivity" to refer to the response to steady illumination. Therefore, the ratio of rod sensitivity with light adaptation operational to the sensitivity with adaptation disabled provides a measure of the extent of adaptation at any given time after the onset of illumination. The approach requires an important baseline to be established: the intensity dependence of the photoresponse amplitude in the absence of light adaptation. A complete description of this baseline state and the method used to establish it are presented in the APPENDIX. Briefly, the relation between the closure of the cGMP-gated channels in response to the destruction of cGMP by light-activated PDE in the absence of any feedback regulation was predicted from:

$$\frac{r(t)}{r_{max}} = 1 - \left(\frac{1}{1 + IF(t)}\right)^{n_{cG}}, \quad (1)$$

where $r(t)/r_{max}$ is the response amplitude divided by the saturated response amplitude, I is the light intensity (measured in photons μm^{-2} s^{-1}), n_{cG} is the Hill coefficient for channel activation by cGMP, and $F(t)$ expresses the fractional degree of PDE activation by a step of light of unit intensity. $F(t)$ was determined from the time integral of the dim flash response (Table I, column 3) as described in the APPENDIX. This baseline relation is represented by the dashed line for $t = 2.5$ s and by the dotted line for $t \geq 9$ s in Fig. 1 B. The positioning on the intensity axis of the predicted curve for the 2.5-s exposures in the absence of feedback differs from that for exposures longer than 9 s by a factor of 0.48 due to the fact that PDE activity had not yet reached the steady state.

The symbols in Fig. 1 B show the response amplitudes observed at three times after the onset of light obtained from Fig. 1 A. The extent of adaptation was found from the magnitude of the rightward shift of the observed response amplitude from the appropriate baseline relation. Deviation was already marked by 2.5 s, when the response peaked, indicating that adaptation began to

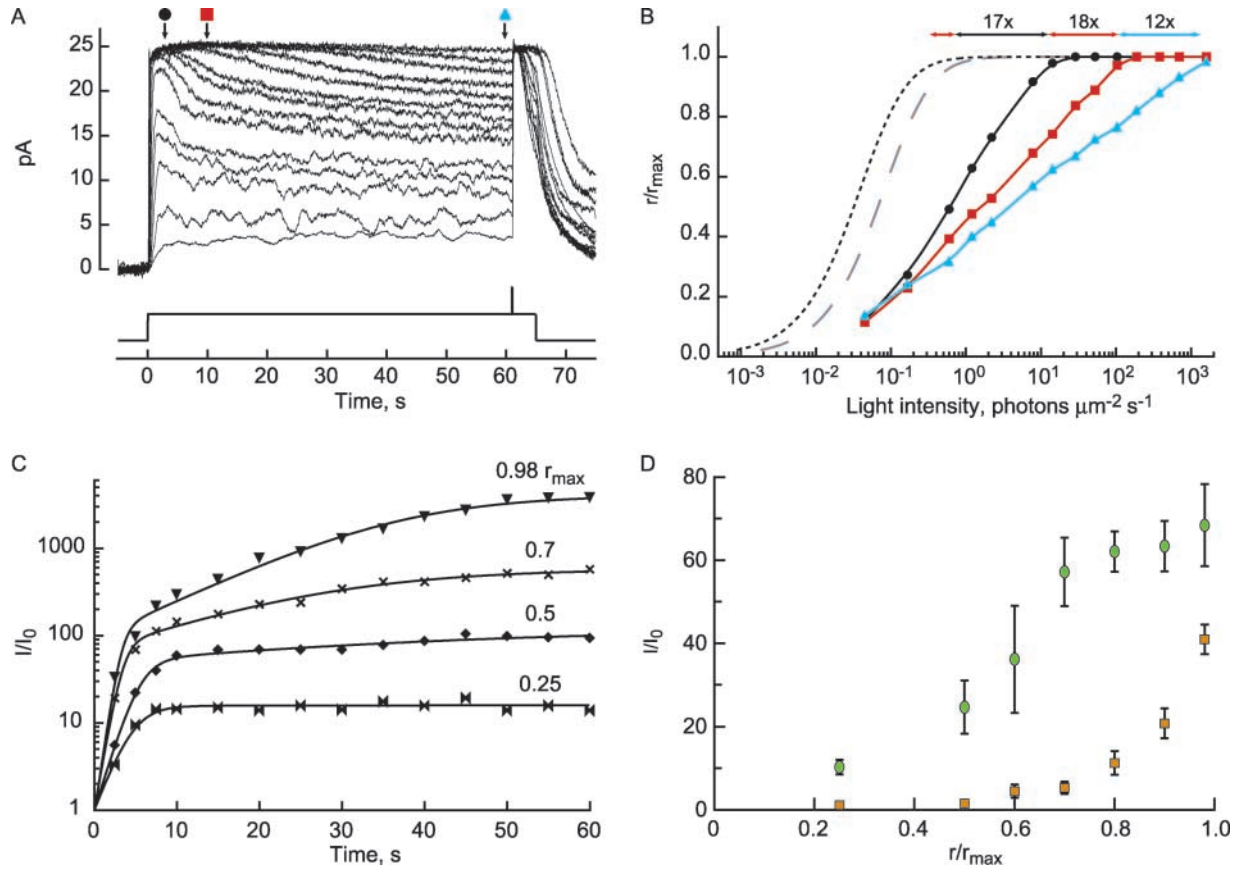

FIGURE 1. Light adaptation in bullfrog rods. (A) Responses of rod 12 to steps of light. Each trace is an average of two or more trials. Output from a photodiode stimulus monitor is shown below the traces. Bright flashes (56–7,500 photons μm^{-2}) were superimposed on the step at 61 s to evaluate the saturating response amplitude. The symbols mark the times at which amplitudes were measured for the analysis presented in B. (B) Progressive adaptation to continuous illumination. Response amplitudes were taken at 2.5 (●), 10 (■, red) or 60 s (▲, blue) after the onset of illumination. The continuous lines through the symbols have no theoretical significance. The dotted and dashed lines predict the relation in the absence of light adaptation (Eq. 1; see APPENDIX). The dashed line represents the responses measured 2.5 s after light onset, whereas the dotted line represents sensitivity determinations at 10 and 60 s. The changes in sensitivity measured at 0.98 r_{max} are shown by the arrows with the desensitization factors listed above each arrow. The magnitude between 2.5 and 10 s (red arrows) includes the magnitude between the dotted and dashed predicted curves. (C) Time course of desensitization for different criterion response amplitudes. Desensitization was estimated as described in B for response levels of 0.98 (▼), 0.70 (×), 0.50 (◆) and 0.25 (⧓) r_{max}. The time points <10 s were corrected for the incomplete activation of PDE where the mean τ_C (3.0 s) was taken as the value of τ_E (see Fig. 7; APPENDIX). Results were fitted with Eq. 2 (continuous lines). (D) Light intensity dependence of the two phases of adaptation. The mean magnitudes of the fast (○, green) and slow (□, orange) phases were found for rods 9, and 11–14 as described in C. Error bars show SEM.

impact the response amplitude nearly immediately after the onset of light. After longer exposures, the slope of the response-intensity relation became progressively flatter, which is consistent with the idea that light adaptation recruits multiple mechanisms that differ in their kinetics and their intensity dependencies.

The full extent of adaptation, as judged by the ratio of the intensities required to elicit a criterion response of 0.98 r_{max} after 60 s of illumination to that predicted for the rod in the absence of adaptation, was quite large. The rod in Fig. 1 was desensitized ~3,700-fold. The average value for seven rods was 3,131 ± 404 (mean ± SEM). We then determined the degree of adaptation after different periods of light exposure (Fig. 1 B). In the ~2.5 s that it took for the step response to reach its peak, the rod in Fig. 1 desensitized ~17-fold. After 10 s, a further ~18-fold loss in sensitivity occurred. An ~12-fold more desensitization operated between 10 and 60 s.

The time course of adaptation during continuous illumination was characterized by extending the analysis shown in Fig. 1 B to include shorter time intervals. In addition, desensitization was determined for other criterion response amplitudes. The ratio of the light intensity required to hold the response at a given criterion level to the intensity required to achieve the same criterion level in the absence of adaptation was plotted as a function of time after light onset (Fig. 1 C). The results of the analysis at each criterion level were fitted with an equation describing the fast and slow adaptation phases as exponen-

TABLE I

Sensitivity Parameters

1	2	3	4	5	6	7	8	9	10	11	12	13	14	15	16	17	18
	Flash responses		Onset of adaptation			τ_C values			Magnitudes					Ca^{2+} exchange current parameters			
Rod	$q_{1/2}$	t_i	τ_{fast}	τ_{slow}	τ_{slow}'	Flash	2.5-s steps	60-s steps	Fast	Slow	Total	ΔT	Slow	a	τ_a	b	τ_b
	hν μm⁻²	*s*	*s*	*s*	*s*	*s*	*s*	*s*				*s*		*1 − r/r_max*	*s*	*1 − r/r_max*	*s*
1	2.2	4.1			9.9	2.1						7.4	51				
2	0.67	4.1			11.7	3.5						8	24	0.110	0.91	0.027	9.6
3	0.91	4.2			9.2	3.5						6.6	12	0.096	0.24	0.056	3.0
4	1	3.4			7.7	2.7						7.4	29	0.120	0.61	0.018	8.4
5	1.3	2.7			6.2	3.8						9	25	0.160	0.57	0.03	3.9
6	0.8	2.8			7.4	3.4						9.8	46	0.240	1.08	0.017	7.6
7	1.4	3.2	0.3	8.0		2.6	2.7	2.5	107	39	4,173	11.1	134	0.080	0.74	0.04	8.1
8	0.95	3.3	0.7	5.2		2.6	2.8	2.5	96	39	3,744	12	175	0.038	0.29	0.093	7.2
9	1.3	3.1	1.2	10.4		2.4	2.5	2	42	41	1,722	10.6	174	0.170	0.19	0.07	3.4
10	0.81	3.4					3.8	2.8				12.4	95	0.110	0.32	0.079	2.9
11	0.43	3.9	0.6	9.8					63	28	1,764						
12	0.55	3.4	0.6	11.0					88	42	3,696						
13	0.46	4.4	0.7	12.6					94	44	4,136						
14	0.45	3.1	1.4	7.4					57	47	2,680						
Mean	0.95	3.5	0.8	9.2	8.7	3.0	3.0	2.5	78	40	3,131	9.4	77	0.125	0.55	0.048	6.0
SEM	0.13	0.1	0.1	0.9	0.9	0.2	0.3	0.2	9	3	404	0.7	20	0.020	0.11	0.009	0.9

(column 2) $q_{1/2}$, the half-saturating flash strength, calculated according to $r/r_{max} = 1 - \exp(-kq)$, where $k = \ln(2)/q_{1/2}$ and q is the flash strength. (column 3) t_i, integration time integral of the dim flash response divided by response amplitude. (columns 4 and 5) τ_{fast} and τ_{slow}', the time constants of the fast and slow phases of light adaptation derived from the 0.98 r_{max} criterion response as explained in Fig. 1 C legend. (column 6) τ_{slow}, time constant for the onset of the slow phase of light adaptation during continuous light determined from the recovery of saturated steps as described in Fig. 4 C legend. (columns 7–9) τ_c, the time constant of the rate-limiting step in the shutoff of phototransduction, estimated from the slope of the relation between saturation time and natural logarithm of either the flash strength or the step intensity. (columns 10–12) Magnitudes of desensitization that operated with fast and slow kinetics and total desensitization during continuous light determined as described in Fig. 1 C legend. (column 13) ΔT, difference in saturation time between the responses to short, 2.5-s steps and long, 80-s (rods 1–6) or 60-s (rods 7–10) steps taken from the brightest intensities applied to both step durations. (column 14) The magnitude of the desensitization that occurred between short and long steps calculated using Eq. 3, ΔT from Col. 13 and τ_c from Col. 7, except for rods 7–9 where the average of the flash and 2.5-s step τ_c values from Cols. 7 and 8 were used and for rod 10 where the 2.5-s step τ_c was used. The magnitudes were corrected for the fractional activation of PDE during the 2.5-s step as explained in the APPENDIX. (columns 15–18) Kinetic parameters of the exchanger current found from a fit of Eq. 4 to responses to saturating steps >25 s in duration.

tial functions and the overall adaptation as the product of those functions (see APPENDIX, Eqs. A20–A23):

$$\frac{I(t)}{I_0} = \frac{(1 + A_1) \cdot (1 + A_2)}{\left[1 + A_1 \exp\left(-\frac{t}{\tau_1}\right)\right] \cdot \left[1 + A_2 \exp\left(-\frac{t}{\tau_2}\right)\right]}, \qquad (2)$$

where $(1 + A_1)$ and $(1 + A_2)$ are magnitudes of desensitization and

$$\frac{I(\infty)}{I_0} = (1 + A_1) \cdot (1 + A_2).$$

This analysis was performed for a total of seven criterion levels, four of which are shown in Fig. 1 C. The fast phase engaged at every criterion level tested, whereas the slow phase was observed only at relatively high criterion levels. At the 0.25-r_{max} criterion level, the rod desensitized in a single fast phase with a time constant of 1.6 s and a magnitude of 13-fold. At the 0.5-r_{max} criterion, a relatively larger 47-fold offset developed with a similar time constant of 1.4 s, but it was followed by a smaller, ~1.5-fold slow desensitization phase with a time constant of ~32 s. At the 0.7-r_{max} criterion, the fast phase amplitude grew to 66-fold with a time constant of 0.8 s, whereas the slow phase reached 8-fold, engaging with a time constant of 13 s. Finally, at the 0.98-r_{max} criterion, the fast phase resulted in 88-fold desensitization with a time constant of 0.6 s, and the slow phase provided 42-fold desensitization with an 11-s time constant. A similar temporal sequence of desensitization was observed in six other rods (Table I, columns 4 and 5). At the 0.98-r_{max} level, the time constant of the fast adaptation phase may only be considered approximate because at time points earlier than ~2 s, the step responses were rising steeply due to rapid changes in the cGMP concentration. This condition precluded the calculation of I_0 by our analysis (see APPENDIX). Yet, it is clear that the fast phase was complete in less than ~5 s after the onset of illumi-

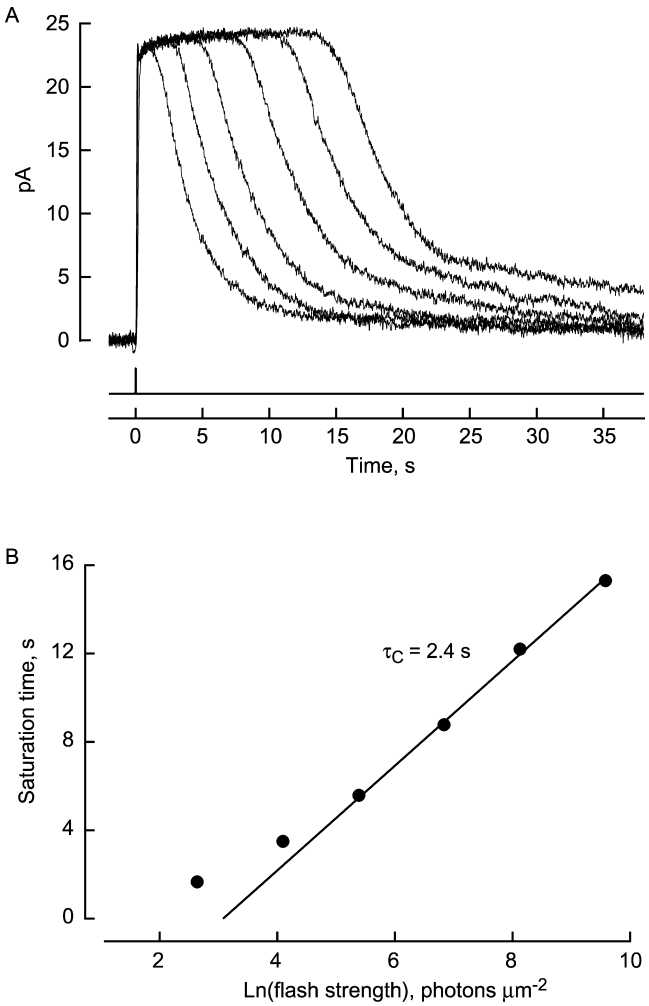

FIGURE 2. Rod saturation times after brief flashes. (A) Responses of rod 9 to flashes. Each trace is the average of two responses. (B) Saturation times plotted as a function of the natural logarithm of the flash strength. Saturation time was measured from mid flash to a criterion recovery of the response to 0.9 r_{max}. Linear regression of the results for flashes of 931 photons μm^{-2} and brighter yielded a recovery time constant of 2.4 s.

nation, and must have had an onset time constant of ~1 s.

The magnitudes of each phase are summarized in Table I (columns 10–12) and in Fig. 1 D, where the degree of rod desensitization due to each phase is plotted as a function of the criterion current suppression level. For the rods analyzed in Fig. 1 D, the fast phase was observed at the lowest response level, virtually saturating at ~70-fold when the steady response reached ~0.8 r_{max}. The slow phase became evident at ~0.5 r_{max} and continued to increase in magnitude through the highest criterion level analyzed surpassing ~40-fold at 0.98 r_{max}.

Recovery from Saturating Light

An alternative method for evaluating the slow phase of light adaptation is based on the analysis of the rod's recovery from saturating light steps. The method is an extension of the approach introduced for the analysis of rod responses to saturating flashes (Pepperberg et al., 1992; Lyubarsky et al., 1996; Nikonov et al., 1998). The behavior of the rod upon stimulation with bright flashes is illustrated in Fig. 2. The photoresponse amplitude saturates with flashes that close all the channels. Further increase in flash strength prolongs the time in saturation (Fig. 2 A). It was posited that once feedback systems that underlie light adaptation during the flash response fully engage, the relationship between the saturation time and the natural logarithm of the flash strength becomes linear with a slope of τ_c reflecting the time constant of the slowest step in the shutoff of the transduction cascade (Pepperberg et al., 1992). This condition appears to be met for saturation times greater than ~6 s in amphibian rods (Fig. 2 B; Pepperberg et al., 1992; Lyubarsky et al., 1996; Murnick and Lamb, 1996).

During the initial recovery from saturating steps, the cascade also appears to shut off exponentially, so a similar analysis may be applied. Fig. 3 A shows the recovery phases of responses of the rod from Fig. 2 to 2.5-s steps of increasing intensity. Saturation time was measured from the moment the light was shut off to a criterion recovery (0.9 r_{max}). For 2.5-s steps where the total time in saturation (including the duration of illumination) was >6–8 s, the relation between saturation time and the natural logarithm of the step intensity increased linearly (Fig. 3 C). The time constant (τ_c) found from the slope of this relation was essentially the same as the value determined from saturating flashes (Fig. 2 B). Thus, the kinetics of the recovery from flashes and short steps appear to be determined by the same rate-limiting biochemical reaction, and 6–8 s of saturation appears to be sufficient to fully engage those adaptation mechanisms that operate under either illumination condition.

We then performed the same analysis with 60-s light steps (Fig. 3, B and C). Only two or three light intensities were used because prolonged exposure of rods to brighter light often caused irreversible losses in sensitivity (not shown). For lights of the same intensity, the saturation time was significantly shorter after the 60-s step compared with that after the 2.5-s step, indicating that a profound loss of sensitivity had occurred during the additional period of light exposure. Nevertheless, the slope of the relation between saturation time and ln(step intensity) for 60-s steps was similar to that obtained for flashes and for short steps (Table I, columns 7–9), which suggests that the slowest cascade shutoff rate was not appreciably changed after prolonged bright steps. Given an invariant slope in the relation between saturation time and ln(step intensity), the magnitude of adaptation occurring between 2.5 and 60 s of illumination was calculated (Lyubarsky et al., 1996):

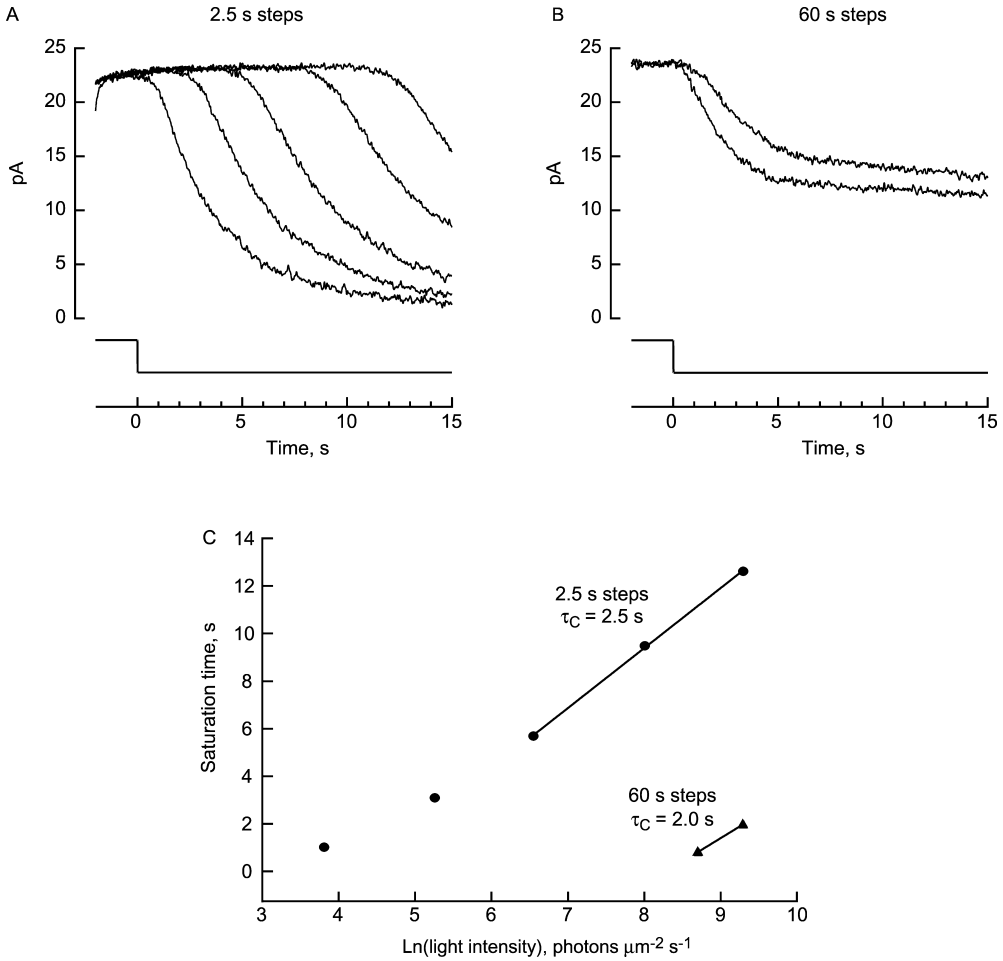

FIGURE 3. Rod saturation times after steps of light. The recovery phases of responses of rod 9 to 2.5- (A) and 60-s (B) light steps. Time zero indicates the moment the light was shut off. (C) Saturation times measured from the moment that the light was shut off to a criterion recovery of the response to 0.9 r_{max} plotted as a function of the natural logarithm of the light intensity. The lines, representing linear regression analyses over the indicated ranges, yielded recovery time constants of 2.5 s and 2.0 s for 2.5- and 60-s steps, respectively.

$$M_S = \exp(\Delta T/\tau_C), \quad (3)$$

where M_S is the fold change in intensity needed to prolong the time in saturation after a 60-s step so that it matched that after a 2.5-s step, and ΔT is the difference in the saturation time after short and long steps of a given intensity (Table I, column 13). Here, the magnitude was divided by $f_0(2.5)$ to adjust for the lower, pre–steady-state PDE* activity engaged during the 2.5-s step (Eq. A5). The average magnitude of the slow phase of light adaptation that operated exclusively during continuous light was 77-fold (Table I, column 14). This method does not include the fractional contribution of the slow phase that may develop within the first 2.5 s of illumination. If the slow phase manifests from the onset of illumination and develops with a time constant of 9.2 s (Table I, column 5), then its magnitude would be 1.3-fold greater. The corrected magnitude of 100-fold provides an estimate for the full extent of desensitization that developed during the slow phase of adaptation because, during supersaturating responses, intracellular Ca^{2+} drops to a minimum. It is somewhat larger than the value of 40-fold estimated by the method in Fig. 1 D (Table I, column 11), where the partial recovery of the response (Fig. 1 A) prevented intracellular Ca^{2+} from falling to such a low level.

The use of saturating steps also provided an independent means for determining the onset kinetics of the slow phase of light adaptation. Saturation times were measured after systematically increasing the duration of a step of constant intensity (Fig. 4). Step intensity was chosen so that the total time in saturation (including step duration) for the shortest step exceeded ~8 s to fully engage the adaptive processes invoked by bright flashes and short steps (see first two paragraphs of this section). As expected, the saturation time initially rose as the step duration increased since PDE activity had not attained steady state. For steps longer than 2.5–10 s, saturation time decreased as the cell desensitized (Fig. 4 B). On average, the time constant of the decline in saturation time was 16.2 ± 0.6 s (mean ± SEM, n = 6).

However, the time constant of the decline in saturation time as determined in Fig. 4 B does not directly correspond to the time constant of the onset of desensitization during the slow phase of adaptation to continuous light. Two considerations must be taken into account. First, saturation time is dependent on the level of PDE* activity at the time the light is shut off. For steps shorter

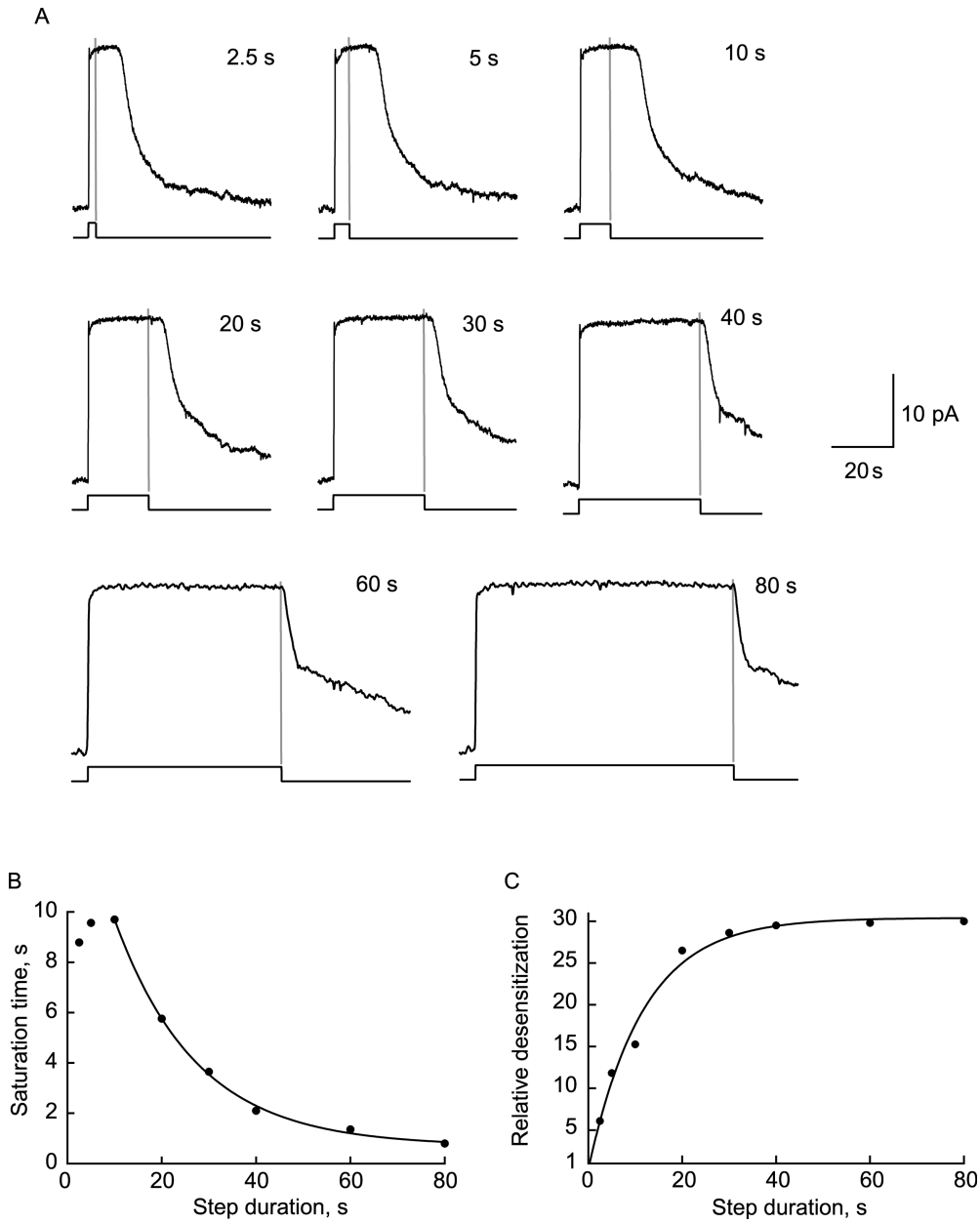

FIGURE 4. Mapping the onset of light adaptation with bright steps of light. (A) Accelerated recovery from saturation after longer light exposure. Each trace shows the average of two responses of rod 2 to a step of 802 photons μm^{-2} s^{-1}. Step durations are given in the top right corner of each panel. The vertical gray lines emphasize the moment at which the light was extinguished for each trace. (B) Time course of the reduction in saturation time. The time required for 10% photocurrent recovery after each light pulse was extinguished is plotted as a function of step duration. The line is a single exponential function with $\tau = 17$ s. (C) Time course of the slow phase of adaptation. The relative sensitivity was calculated from the difference in saturation time (ΔT) between the 80-s step and that at the indicated step duration and the τ_C from flash responses according to Eq. 3. For steps of <10-s duration, the relative sensitivities were divided by f_0(step duration) (see APPENDIX, Eq. A5), where τ_E was taken as $\tau_C = 3.5$ s measured for this cell to account for fractional, pre–steady-state PDE activity, and fitted with a single exponential with $\tau = 12$ s. The results were expressed as desensitization relative to the amplitude of the exponential at time zero.

than ~9 s, the duration of illumination was insufficient to allow PDE* activity to reach a steady state (see APPENDIX). This led to an underestimation of the degree of adaptation occurring between short and long steps because, even in the absence of light adaptation, the lower PDE* activity at the end of a short step reduced saturation time relative to that after a longer step of the same intensity. Second, sensitivity is actually an exponential function of the change in the saturation time (Eq. 3). To account for both factors, ΔT was taken as the difference between the saturation time for each step duration and that for the 80-s step, and the relative sensitivities were calculated according to Eq. 3. Then, for each step duration, the relative sensitivity was divided by a factor f_0(step

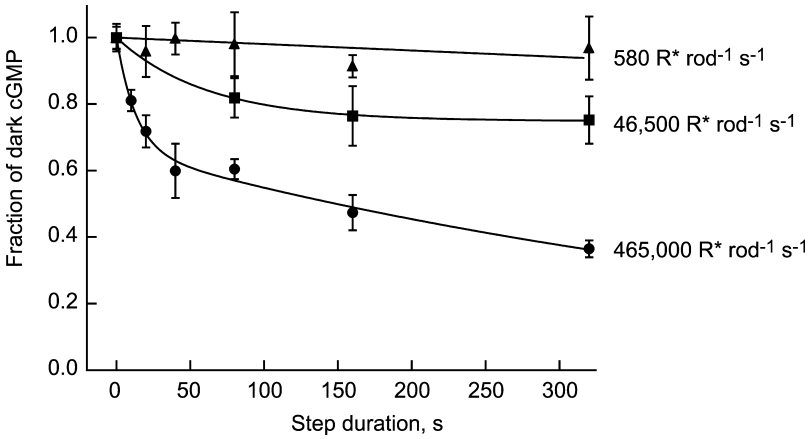

FIGURE 5. cGMP dissociation from the noncatalytic binding sites on PDE. The cGMP levels of cryodissected rod outer segments were determined in dark-adapted samples or in samples exposed to steady illumination at three different intensities (given on the right) as described in MATERIALS AND METHODS. Each data point is the average of at least four determinations. Error bars represent the SEM. The line through the triangles is a linear regression; the slope did not differ significantly from zero. The line through the squares is a fitting with a single exponential, $\tau = 62.5$ s. The line through the circles is a fitting with the sum of two exponentials: $a = 0.34$, $\tau_a = 13$ s; $b = 0.66$, $\tau_b = 532$ s.

duration) to correct for PDE* activity (see APPENDIX, Eq. A5). The desensitization relative to that of the dark-adapted state (time = 0) was plotted as a function of step duration as shown in Fig. 4 C. The mean time constant for six rods was 8.7 s (Table I, column 6). This value was similar to the time constant of the slow adaptation phase of 9.2 s determined from the analysis of step response families (Fig. 1 C; Table I, column 5).

cGMP Dissociation from Noncatalytic Sites on PDE in Physiologically Active Rods

It has been proposed that T*–PDE* shutoff accelerates during light adaptation as cGMP dissociates from noncatalytic sites on PDE (Arshavsky et al., 1991; Arshavsky and Bownds, 1992; Calvert et al., 1998). The time course of cGMP dissociation from T-activated PDE in isolated rod outer segments is biphasic (Cote et al., 1994; Yamazaki et al., 1996; Calvert et al., 1998), and the time constant of the faster phase is similar to the onset of the slow phase of light adaptation characterized in the present work. However, it was not clear whether cGMP dissociated in an appropriate light-dependent manner in intact, physiologically active rods (compare with de Azeredo et al., 1981; Govardovskii and Berman, 1981; Blazynski and Cohen, 1986; Cohen and Blazynski, 1988, 1993). Therefore, we tested the hypothesis that this mechanism could be responsible for the slow phase of adaptation by comparing the rate and intensity dependence of cGMP dissociation from these sites in intact retinas with the rate and intensity dependence of the slow phase of adaptation. Flat-mounted samples of isolated, dark-adapted retina were kept in darkness or exposed to continuous light of various durations and intensities and were rapidly frozen. Rod outer segments were collected with a cryomicrotome and their cGMP content quantified by radioimmunoassay.

About 95% of cGMP in the outer segment of a dark-adapted rod is bound to the noncatalytic sites on PDE (Cote and Brunnock, 1993). So nearly the entire light-induced decline in cGMP is due to its dissociation from these sites and its subsequent hydrolysis. Fig. 5 shows the time course of light-dependent cGMP decline in ROS of physiologically active retinas exposed to constant light producing 580, 46,500, or 465,000 R* rod^{-1} s^{-1}. For the brightest intensity, 30% of the cGMP dissociated with a time constant of 13 s, whereas the remainder dissociated with a time constant of 532 s. The kinetics of cGMP decline at the brightest light level was similar to that reported for transducin-activated PDE in isolated ROS (Cote et al., 1994; Yamazaki et al., 1996; Calvert et al., 1998). These results contrast with those reported by Cohen and Blazynski (1988, 1993) and Blazynski and Cohen (1986) who used an approach similar to ours; the basis for the difference is not known.

Although the first phase of cGMP dissociation in bright light developed with a time course similar to the onset of the slow adaptation phase, the intensity of light required for cGMP dissociation was much higher than that causing the adaptation. For the rod in Fig. 1, the slow phase of light adaptation was detectable during illumination delivering 2.2 photons μm^{-2} s^{-1}, the intensity that half-saturated the rod's photoresponse after 60 s of illumination. The collecting area (Baylor et al., 1979b) of this rod, calculated from measurements of the dimensions of its outer segment (7-μm diameter and 57-μm length) was 27 μm^2, so this intensity produced ~60 R* s^{-1}. The half-saturating step intensities for rods 9 and 11–14 produced 88 ± 38 (mean ± SEM) R* s^{-1}. In contrast, cGMP dissociation from the noncatalytic sites on PDE was undetectable during illumination producing ~600 R* s^{-1}. Therefore, cGMP feedback onto T*–PDE* lifetime through this mechanism cannot be the basis for the slow phase of adaptation.

Estimation of the Kinetics of Light-induced Ca^{2+} Decline

Most feedback reactions known to underlie light adaptation are mediated by the light-dependent decline in intracellular Ca^{2+} (for review see Pugh et al., 1999). We next examined the intracellular Ca^{2+} dynamics to see whether a component of Ca^{2+} decline correlated with

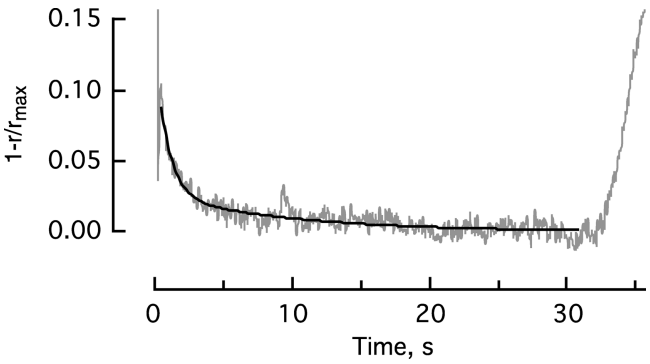

FIGURE 6. $Na^+/K^+,Ca^{2+}$ exchanger current kinetics. The noisy trace is the inverted response of rod 2 to a 30-s step of light (802 photons μm^{-2} s^{-1}). r_{max} was 28.3 pA. The last 10–15% of the circulating current to be suppressed in the photoresponse is carried by the $Na^+/K^+,Ca^{2+}$ exchanger and reflects the rate of light-dependent Ca^{2+} decline. The smooth line shows a fit to the sum of two exponentials (Eq. 4) where $\alpha = 0.11$, $\tau_a = 0.91$ s, $b = 0.03$, $\tau_b = 9.6$ s.

the slow phase of adaptation. The dark current in a rod is the sum of the currents carried by the cGMP-gated channel and by the electrogenic $Na^+/K^+,Ca^{2+}$ exchanger (Yau and Nakatani, 1984). The cGMP-gated channels close quickly after bright saturating stimuli, leaving a residual current carried by the exchanger. The stoichiometry of cation movement is fixed, where there is a net movement of one positive charge inward for each Ca^{2+} ion removed (Lagnado and McNaughton, 1991). The exchanger operates linearly over the physiological Ca^{2+} concentration range (Lagnado et al., 1992), and the exchanger current closely reflects the kinetics of the decline of intracellular Ca^{2+} (Gray-Keller and Detwiler, 1994; McCarthy et al., 1996). Therefore, we measured the current carried by the $Na^+/K^+,Ca^{2+}$ exchanger after the onset of bright steps that kept the rod in saturation for at least 25 s.

Fig. 6 shows the $Na^+/K^+,Ca^{2+}$ exchanger current recorded from rod 2 (noisy trace). The response was inverted and normalized to the total suppressible current. The smooth line represents the fitting of the current with the sum of two exponentials:

$$1 - \frac{r(t)}{r_{max}} = a \cdot \exp(-t/\tau_a) + b \cdot \exp(-t/\tau_b). \qquad (4)$$

On average, ~70% of the fall in Ca^{2+} occurred with a time constant of 0.55 s, and the remaining 30% occurred with a time constant of 6.0 s (Table I, columns 15–18). These results are in good agreement with a previous report where both exchange current kinetics and the kinetics of Ca^{2+} decline made using Ca^{2+}-sensitive dyes were studied in frog (McCarthy et al., 1996). They indicate that Ca^{2+} is declining during the onset of the slow phase of light adaptation, and raise the possibility that a Ca^{2+}-dependent mechanism is involved.

DISCUSSION

Upon exposure to steady illumination, bullfrog rods light adapt in at least two temporally distinct phases. One phase develops within seconds after the onset of light. It results in a progressive desensitization of the rod with increasing ambient light intensity, reaching ~80-fold with near-saturating intensities. The second phase evolves much more slowly and operates at higher intensities, appearing with light steps that suppress more than ~50% of the circulating current. Desensitization imparted by the slow phase may approach ~100-fold. The fast phase has been analyzed previously (for review see Pugh et al., 1999). The slow phase that manifests as a partial recovery of the circulating current during near saturating light steps has been observed previously (Dowling and Ripps, 1972; Fain, 1976; Baylor et al., 1980; Forti et al., 1989; Matthews, 1990; Koutalos et al., 1995b) but not analyzed quantitatively. What mechanisms underlie each phase?

In principle, light adaptation could involve modulation of R* formation, R* and PDE* catalytic activities, R* and PDE* lifetimes, guanylate cyclase activity, and the channel's affinity for cGMP (for reviews see Bownds and Arshavsky, 1995; Pugh et al., 1999; Pugh and Lamb, 2000; Burns and Baylor, 2001; Fain et al., 2001). The overall extent of desensitization is given by the product of the relative changes in each parameter (see APPENDIX, Eqs. A17–A19). Some of these changes are known to operate during light adaptation through Ca^{2+}-dependent mechanisms. The contribution of others are, at present, either disputed or not currently implicated.

The fast phase of light adaptation is Ca^{2+}-dependent because it is not present when the light-induced Ca^{2+} decline is inhibited (Matthews et al., 1988; Nakatani and Yau, 1988). It consists of two components: one that operates on "early" or upstream components of the rod phototransduction cascade, and another that operates on "late" or downstream cascade components (Matthews, 1996). The component that operates upstream in the cascade, which may be viewed as a reduction in the potency of light to activate PDE, probably involves Ca^{2+} regulation of R* lifetime (Matthews et al., 2001) through Ca^{2+}-recoverin inhibition of rhodopsin kinase since it is not present in rods of transgenic mice lacking recoverin (Dodd, 1998). It provides as much as a 10-fold desensitization after bright flashes (Murnick and Lamb, 1996). The onset kinetics of the upstream component may be determined from the responses to saturating probe flashes presented with varying delay after a bright, saturating conditioning flash as described by Murnick and Lamb (1996). They showed that the saturation time of the probe flash response declined exponentially as a function of the flash separation time with a time constant of ~2.4 s. The onset rate of the upstream component, given by the reduction in sensitivity

that is nonlinearly related to the saturation time, would be about twofold faster (as estimated with Eq. 3).

The components of the fast adaptation phase that operate downstream in the cascade, likely mediated by Ca^{2+}-dependent modulations of guanylate cyclase and the cGMP-gated channel, engage with a time constant of ~1 s (Matthews, 1996) and provide a 14–19-fold decrease in sensitivity (Lyubarsky et al., 1996; Matthews, 1996). Combined, the upstream and downstream components of the fast adaptation phase reported by these authors provide as much as 190-fold desensitization. Our estimate of 70-fold for the magnitude of the fast phase was somewhat smaller, probably due to intrusion of the slow phase in the previous studies and to the imperfect separation of the two phases by the methods in the present study. Our analysis assumes that the slow phase of adaptation begins to operate from the onset of illumination, which may not be the case.

The slow phase of adaptation is unlikely to consist simply of the continued operation of feedbacks onto guanylate cyclase and the cGMP-gated channels on a slower time scale. If this were the case, the time course of adaptation to saturating flashes would be roughly the same as that to continuous light. A step of light that produces 0.98 r_{max} (Fig. 1 C) resulted in an ~300-fold reduction of sensitivity in 12 s, whereas bright flashes that kept responses in saturation for ~12 s resulted in a modest 14-fold desensitization as estimated from the leftward shift in the relation between saturation time and flash strength when Ca^{2+} feedback was inhibited (Lyubarsky et al., 1996). The 20-fold extra desensitization observed during continuous activation of the phototransduction cascade by a step of light, which is absent after transient cascade activation by a flash, implicates a target for the slow phase of adaptation within the primary excitatory pathway, R* → T* → PDE*.

We considered whether the slow adaptation phase could be mediated by regulation of the lifetime of T*–PDE*. The only putative feedback regulation of T*–PDE* lifetime described to date involves the acceleration of transducin GTPase upon the dissociation of cGMP from noncatalytic binding sites on PDE (Arshavsky et al., 1991). We directly ruled out this mechanism by showing that cGMP dissociates from these sites in intact rods on the retina only at light intensities much brighter than required to observe the slow adaptation phase. This conclusion is supported by the apparent invariance of short and long step τ_Cs (Fig. 3 and Table I, columns 8 and 9) and the lack of significant change in flash τ_C in the presence of background light (Pepperberg et al., 1994; Nikonov et al., 2000). The rate of T*–PDE* shutoff is thought to set the τ_C in amphibian rods (Lyubarsky et al., 1996) so a substantial shortening of T*–PDE* lifetime would lead to a dramatic reduction in τ_C.

Another possibility is that the slow phase is mediated by a reduction in the efficiency of R* to increase the rate of cGMP hydrolysis. This could occur by a reduction of R* lifetime, a reduction of the efficiency of T* to activate PDE or by a reduction in R* or PDE* catalytic activities. Nikonov et al. (2000) showed that adapting lights that suppressed up to 80% of the circulating current did not alter the very initial trajectories of flash responses. Since the initial trajectory is dependent on the rates of PDE activation and cGMP hydrolysis by the activated PDE (Lamb and Pugh, 1992), this result appears to rule out regulation of the efficiency of T* activation of PDE and the catalytic activities of R* and PDE* for responses $<0.8\ r_{max}$. By exclusion, regulation of R* lifetime emerges as the best candidate within this response range. The brief lifetime of R*, which disappears with a time constant <0.5 s after photon absorption (Matthews, 1997; Nikonov et al., 1998), explains why this mechanism produces little adaptation after transient cascade activation by a flash, but may become much more potent during continuous cascade activation by a light step. Ca^{2+}-recoverin is the only species demonstrated to regulate R* lifetime (Kawamura, 1993; Chen et al., 1995; Klenchin et al., 1995) and the continued decline in Ca^{2+} during the development of the slow adaptation phase raises the possibility that the slow phase is Ca^{2+}-dependent. However, the magnitude of Ca^{2+}-recoverin regulation of rhodopsin kinase activity, three- to fivefold (Calvert et al., 1998; Nikonov et al., 2000), appears insufficient.

At intensities suppressing >80% of the circulating current, the mechanism of the slow phase may not be restricted to regulation of R* lifetime, allowing once again the possibility of regulation of the efficiency of T* to activate PDE and of R* or PDE* catalytic activity. Some prospective mechanisms for the regulation of T*–PDE*/PDE* interaction include PDEγ phosphorylation (Tsuboi et al., 1994; Xu et al., 1998) and/or ADP ribosylation (Bondarenko et al., 1997, 1999). Korschen et al. (1999) have shown that an interaction of PDE* with GARP2, a glutamic acid–rich protein, reduces its catalytic activity. Each of these mechanisms would reduce the total PDE* activity, but their magnitudes under physiological conditions are not yet known. It remains to be seen if there is any Ca^{2+}-dependent regulation of light-stimulated PDE activity. Evidence for Ca^{2+}-dependent regulation of R* catalytic activity has been presented (Lagnado and Baylor, 1994).

A salient feature of the slow adaptation phase is its threshold-like appearance. It is virtually absent from responses to dim light steps, appearing only with light that suppresses 50% or more of the circulating current. This result suggests that the slow adaptation phase, if indeed dependent on Ca^{2+} decline, is mediated by a Ca^{2+} regulatory protein with a fairly high binding coop-

erativity and rather low $K_{1/2}$ relative to the Ca^{2+} level in the dark-adapted rod outer segment cytoplasm. The goal of future experiments will be to determine whether or not the slow adaptation phase is truly Ca^{2+}-dependent and to identify the molecular targets and the feedback regulators that underlie this process.

APPENDIX

Here, our goal is to show how the extent of light adaptation may be extracted from a series of responses to steps of light and to express it in terms of feedback regulation of phototransduction cascade components. We begin by formally describing the rod response to a step of light in the absence of feedback reactions (the "no adaptation" case; Eq. 1). We then explain how the no adaptation response can be predicted based on experimental data obtained with operational feedbacks. Finally, we show how the different parameters of the phototransduction cascade could contribute to adaptation. Many of the equations appearing in this Appendix have been obtained previously (Hodgkin and Nunn, 1988; Forti et al., 1989; Matthews et al., 1990; Tamura et al., 1991; Koutalos et al., 1995b). For comparative purposes, we shall use the most recent notation and equations developed by Nikonov et al. (2000) wherever possible. Henceforth, their derivation will be referred to as NLP.

The concentration of cGMP, the molecule that controls the light-sensitive conductance of the ROS plasma membrane, is set by the balance between its synthesis by guanylate cyclase $\alpha(t)$ and its hydrolysis by PDE $\beta(t)$ (Hodgkin and Nunn, 1988):

$$\begin{aligned}\frac{dcG(t)}{dt} &= \alpha(t) - cG\cdot\beta(t)\\ &= \alpha(t) - cG\cdot(\beta_d + \beta_s(t)),\end{aligned} \tag{A1}$$

where $\alpha(t)$ and $\beta(t)$ are expressed per unit volume of the ROS cytoplasm and $\beta(t)$ is the sum of the dark PDE activity β_d and the light-stimulated PDE activity β_s(t). Our Eq. A1 is essentially NLP's Eq. A3. For completeness, the exchange of free cGMP with that bound to noncatalytic sites on PDE and to cGMP-gated channels should be included in Eq. A1. However, the rate of release of cGMP from PDE sites is low compared with the guanylate cyclase activity, and cannot contribute significantly to the balance of free cGMP. For instance, the saturating background light producing 46,500 R* s^{-1} results in the release of cGMP from PDE sites at the rate of 0.4% of its dark content per second, or ~0.8 μM s^{-1} (Fig. 5). At the same time, the saturating background results in a cGMP flux of 12–30 μM s^{-1} (Calvert et al., 1998; Nikonov et al., 2000), but which may be as high as 100 μM s^{-1} (Dawis et al., 1988). The total amount of cGMP bound to the channels is simply too low to have any effect. Thus, we neglect the release of cGMP bound to PDE noncatalytic sites and to the channel from further consideration of dcG(t)/dt.

At the peak and the plateau of the steady response,

$$\frac{dcG(t)}{dt} = 0,$$

and during the slow phase of adaptation,

$$\frac{dcG(t)}{dt} \ll \alpha(t), cG\cdot\beta(t).$$

Therefore,

$$cG(t) \approx \frac{\alpha(t)}{\beta(t)}. \tag{A2}$$

The quasi–steady-state Eq. A2 can be applied to times from the peak of the response onward. It is not applicable to the steeply rising front of the response where the complete differential Eq. A1 should be solved.

The cGMP hydrolytic activity elicited by a light step of intensity I (measured in photons μm^{-2} s^{-1}) in the absence of feedback is

$$\beta_{s0}(t) = I\cdot A_c\cdot\beta_{\infty 0}\cdot f_0(t), \tag{A3}$$

where the subscript 0 denotes the value in the absence of light adaptation,

$$\beta_\infty = \frac{\nu_{RE}\cdot\beta_{sub}}{k_R\cdot k_E} = \nu_{RE}\cdot\tau_R\cdot\tau_E\cdot\frac{0.5(k_{cat}/K_m)}{N_{AV}\cdot V_{cyto}}, \tag{A4}$$

$$f(t) = 1 - \frac{k_R\cdot\exp(-k_E\cdot t) - k_E\cdot\exp(-k_R\cdot t)}{k_R - k_E}. \tag{A5}$$

Here β_∞ denotes the final steady level of hydrolytic activity elicited by continuous light producing 1 R*s^{-1}, A_c is the ROS light collecting area (measured in μm^2), ν_{RE} is the steady-state rate of PDE activation in a rod produced by one R* s^{-1}, k_R ($=1/\tau_R$) is the rate constant of rhodopsin quenching, k_E ($=1/\tau_E$) is the rate constant of PDE* shutoff, β_{sub} is the rate constant of cGMP hydrolysis by a single PDE* catalytic subunit of which there are two per enzyme unit (compare with NLP's Eq. A8), k_{cat} is the maximum rate of cGMP hydrolysis by a PDE enzyme unit, K_m is the PDE Michaelis constant, N_{AV} is Avogadro's number, and V_{cyto} is the ROS cytoplasmic volume. Eqs. A3 and A5 were obtained from the integration of NLP's Eqs. A1 and A2. Eq. A4 follows from NLP's Eq. A11. *f(t)* describes the PDE* activity, relative to that at steady-state, as a function of time after light onset.

Relating step-induced PDE activity to the circulating current flowing into the ROS, i:

$$\begin{aligned} i &\approx i_m\cdot\left(\frac{cG}{K_{cG}}\right)^{n_{cG}}\\ &= i_m\cdot\left[\frac{\alpha}{K_{cG}(\beta_d + \beta_s(t))}\right]^{n_{cG}},\end{aligned} \tag{A6}$$

where i_m is the maximum possible current when all channels are open, K_{cG} is the dissociation constant of cGMP from the channels, and n_{cG} is Hill's coefficient (NLP, Eq. 1). In the absence of any evidence to the contrary, we assume that the cooperativity of cGMP binding to the channel is unaffected by light adaptation, i.e., $n_{cG} = n_{cG0}$. However, α and K_{cG} are subject to feedback during light adaptation. The magnitude of the current flowing in darkness (i_d) is

$$i_d \approx i_m\left(\frac{\alpha_0}{K_{cG_0}\cdot\beta_d}\right)^{n_{cG}}, \tag{A7}$$

and the fractional circulating current after light stimulation is the ratio of Eq. A6 to Eq. A7,

$$\frac{i(t)}{i_d} \approx \left(\frac{\alpha}{\alpha_0}\cdot\frac{K_{cG_0}}{K_{cG}}\cdot\frac{1}{1+(\beta_s(t))/\beta_d}\right)^{n_{cG}}. \tag{A8}$$

In the absence of light adaptation, the fractional response to a given step intensity I is

$$\frac{r_0(t)}{r_{max}} = 1-\frac{i_0(t)}{i_d} = 1-\left(\frac{1}{1+\beta_{s_0}(t)/\beta_d}\right)^{n_{cG}}. \tag{A9}$$

Note that I is a part of $\beta_{s0}(t)$ (Eq. A3). Eq. A9 can be rewritten as

$$\frac{r_0(t)}{r_{max}} = 1-\left(\frac{1}{1+I\cdot F(t)}\right)^{n_{cG}}, \tag{A10}$$

where $F(t)$ is a sensitivity factor,

$$F(t) = A_c\frac{\beta_{\infty 0}}{\beta_d}\cdot f_0(t), \tag{A11}$$

expressing the fractional degree of PDE activation by a step of light of unit intensity. Eq. A10 is identical to Eq. 1. Equations of this form have been derived previously (Forti et al., 1989; Matthews et al., 1990; Tamura et al., 1991; Koutalos et al., 1995b).

In principle, the relation between $r_0(t)/r_{max}$ and I may be found experimentally from physiological recordings during inhibition of Ca^{2+} feedback reactions. Unfortunately, direct determination of F in our experiments was not possible because of technical problems in inhibiting Ca^{2+} decline in frog rods. The ciliary connection between the inner and outer segments in frog rods is quite fragile and tended to break when exposed to the flow of feedback-inhibiting solution. Moreover, responses of isolated rods were distorted by the small current carrying capacity of the inner segment, which was largely saturated by the dark current level. Yet, we selected bullfrogs for these experiments expressly to compare the physiology with the well characterized biochemistry in general, and more specifically, with the kinetics of cGMP dissociation from the noncatalytic binding sites on PDE in intact rods. Therefore, an alternative method to find $F(t)$ was used.

In the linear response range ($r_0(t)/r_{max} \ll 1$), Eq. A10 becomes

$$\frac{r_0(t)}{r_{max}} = n_{cG}\cdot I\cdot F(t). \tag{A12}$$

On the other hand, the step response is equal to the product of the light intensity and the time integral of $S_0(t)$, the fractional single photon response in the absence of feedback regulation:

$$\frac{r_0(t)}{r_{max}} = I\cdot A_c\cdot\int_0^t S_0(t)\,dt. \tag{A13}$$

The steady response (at $t=\infty$) is

$$\begin{aligned}\frac{r_0(\infty)}{r_{max}} &= I\cdot A_c\cdot\int_0^\infty S_0(t)\,dt\\ &= I\cdot A_c\cdot S_{m0}\cdot t_{i0},\end{aligned} \tag{A14}$$

where S_{m0} is the amplitude, and t_{i0} is the integration time of the normalized single photon response. Combining Eqs. A12–A14,

$$\begin{aligned}F(t) &= \frac{A_c}{n_{cG}}\int_0^t S_0(t)\,dt\\ &= \frac{A_c\cdot S_{m0}\cdot t_{i0}}{n_{cG}}f_0(t),\end{aligned} \tag{A15}$$

and the steady level of $F(t)$ is

$$F(\infty) = \frac{A_c\cdot S_{m0}\cdot t_{i0}}{n_{cG}}. \tag{A16}$$

Thus, the sensitivity factor F that relates the "no adaptation" step response to stimulus intensity can be obtained from a flash response in the linear range during inhibition of Ca^{2+} feedback.

To estimate F, we recorded dim flash responses of individual frog rods in normal Ringer's solution. We multiplied the response integrals by a correction factor derived from the ratio of dim flash response areas recorded in the presence and absence of Ca^{2+} feedback inhibition from rods of species more amenable to these sorts of experiments. The effect of inhibiting Ca^{2+} feedback on the kinetics and sensitivity of dim flash responses has been studied extensively in the rods of the tiger salamander (Matthews et al., 1988; Fain et al., 1989; Nikonov et al., 1998) and toads (Rieke and Baylor, 1996). The ratio of dim flash response areas recorded in the presence and absence of Ca^{2+} feedback inhibition from these studies ranged from 5.7 to 11. We adopted the value of 5.7 from toad because their ROS dimensions and the response properties of their rods in normal Ringer's were most similar to those of bullfrog rods. If instead the value of 11 was selected, then the "no adaptation" response-intensity relation would

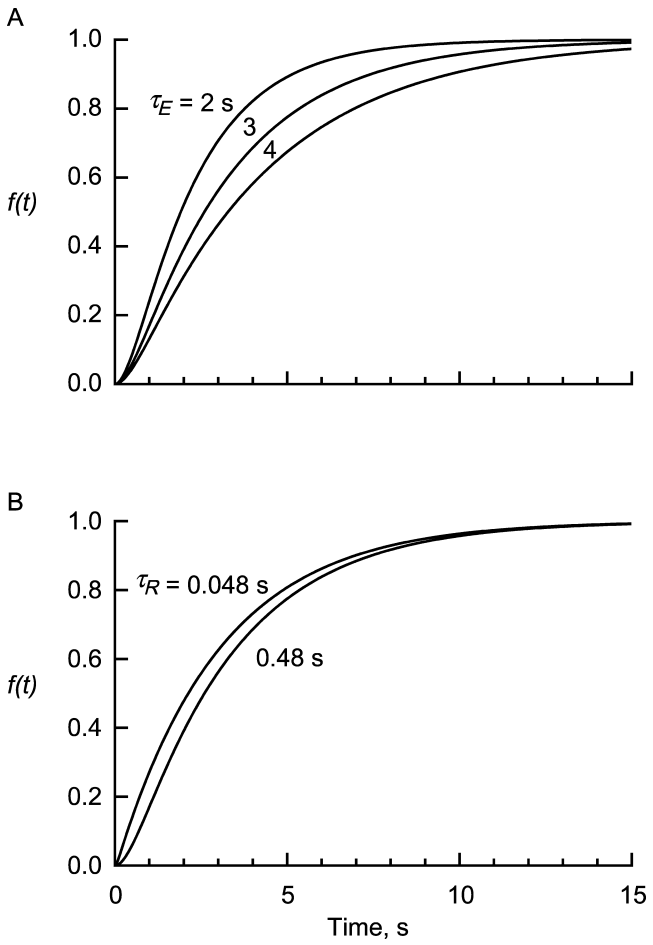

FIGURE 7. Onset of PDE activity in response to steady light. The transition of PDE activity from the dark to the steady-state level activated by the onset of continuous light at time zero, was calculated from Eq. A5. (A) Dependence of the transition on τ_E, τ_R = 0.48 s. (B) The effect of a 10-fold change in τ_R on the time course, τ_E = 3 s.

shift to lower intensities and the magnitude of adaptation would increase 1.9-fold.

To assess the magnitude of adaptation early in the step response, there is an additional consideration. After a step change in illumination, the overall PDE activity reaches a steady level relatively slowly, due to the slow time constant of PDE shutoff, τ_E. The term $f(t)$ from Eq. A5 with sufficient accuracy approaches the steady level of 1 for $t > 3\tau_E$ (Fig. 7). In our analysis, τ_R was assigned the value of 0.48 s (Nikonov et al., 1998), and τ_C was taken as an estimate of τ_E (Lyubarsky et al., 1996). The values we obtained for τ_C ranged from 2.1 to 3.8 s, the mean value being 3.0 s (Table I, column 7). However, note that τ_R and τ_E enter Eqs. A4 and A5 symmetrically, so it is not important to which time constant a particular value is assigned. The time courses of $f(t)$ for τ_E values of 2, 3, and 4 s are illustrated in Fig. 7 A. Variation in the magnitude of τ_R had a much smaller effect (Fig. 7 B). This means that the steady level of $F(\infty) = A_c \cdot S_{m0} \cdot t_{i0}/n_{cG}$ can only be used for $t \geq 9$ s. To predict the relation between the no adaptation response and intensity at times earlier than 9 s, it was necessary to estimate the transient term that depends on both τ_E and τ_R. For example, at $t = 2.5$ s, $f = 0.48$.

The ratio of the intensity required to elicit any given fractional response to the intensity required to elicit the same response (leaving the same circulating current) in the absence of adaptation provides a measure of the extent of adaptation. Let us express it in terms of the parameters of the phototransduction cascade. From Eq. A8, the light intensity I that results in a certain fixed level of circulating current i is

$$I = \frac{\beta_d}{A_c \cdot \beta_\infty \cdot f(t)} \cdot \left[\frac{\alpha}{\alpha_0} \cdot \frac{K_{cG_0}}{K_{cG}} \cdot \left(\frac{i_d}{i}\right)^{1/n_{cG}} - 1\right], \qquad \text{(A17)}$$

where I is of course a function of time. Thus,

$$\frac{I}{I_0} = \left(\frac{\beta_{\infty 0} \cdot f_0(t)}{\beta_\infty \cdot f(t)}\right) \cdot \frac{\left(\frac{\alpha}{\alpha_0}\right) \cdot \left(\frac{K_{cG_0}}{K_{cG}}\right) \cdot \left(\frac{i_d}{i}\right)^{1/n_{cG}} - 1}{\left(\frac{i_d}{i}\right)^{1/n_{cG}} - 1} \quad . \qquad \text{(A18)}$$

Since we are considering intensities resulting in the same response amplitude, $i = i_0$. In the steady state, and for bright stimuli where $i_d/i \gg 1$, Eq. A18 simplifies to

$$\begin{aligned} \frac{I}{I_0} &= \left(\frac{\alpha}{\alpha_0}\right) \cdot \left(\frac{K_{cG_0}}{K_{cG}}\right) \cdot \left(\frac{\beta_{\infty 0}}{\beta_\infty}\right) \\ &= \left(\frac{\alpha}{\alpha_0}\right) \cdot \left(\frac{K_{cG_0}}{K_{cG}}\right) \cdot \left(\frac{\nu_{RE_0} \cdot \tau_{R_0} \cdot \tau_{E_0} \cdot k_{cat_0}}{\nu_{RE} \cdot \tau_R \cdot \tau_E \cdot k_{cat}}\right). \end{aligned} \qquad \text{(A19)}$$

A similar equation was derived by Koutalos et al. (1995b). Eq. A19 gives the extent of adaptation as the product of the degree of guanylate cyclase activation, the degree of modulation of the channel's affinity for cGMP and the modulation of the light-induced cGMP hydrolysis. The latter, in turn, is the product of the modulations of the catalytic activity of R*, R*, and PDE* lifetimes and PDE* catalytic activity proper. The possible contribution of each of these factors to overall light adaptation is evaluated in the DISCUSSION.

We can now justify the form of Eq. 2 used to characterize the time course of adaptation. Let us consider the Ca^{2+} feedback onto guanylate cyclase. From NLP's Eq. A10 and Eq. A16 of Forti et al. (1989),

$$\begin{aligned} \alpha &= \alpha_{min} + \frac{\alpha_{max} + \alpha_{max}}{1 + (Ca/K_{cyc})^{n_{cyc}}} \\ &\approx \frac{\alpha_{max}}{1 + (Ca/K_{cyc})^{n_{cyc}}}, \end{aligned} \qquad \text{(A20)}$$

where Ca is the cytoplasmic Ca^{2+} concentration, K_{cyc} is the half-inhibition constant of cyclase, and n_{cyc} is Hill's

coefficient for the regulation. α_{min} can be neglected in Eq. A20 since $\alpha_{max} \gg \alpha_{min}$ (Koutalos et al., 1995a; Calvert et al., 1998; Nikonov et al., 2000). In darkness,

$$\alpha_0 = \frac{\alpha_{max}}{1 + (Ca_0/K_{cyc})^{n_{cyc}}}. \quad \text{(A21)}$$

The degree of activation of guanylate cyclase at any given moment is

$$A = \frac{\alpha}{\alpha_0} = \frac{1 + (Ca_0/K_{cyc})^{n_{cyc}}}{1 + (Ca(t)/K_{cyc})^{n_{cyc}}} = \frac{A_{max}}{1 + (Ca(t)/K_{cyc})^{n_{cyc}}}. \quad \text{(A22)}$$

A_{max} may be thought of as the degree of suppression of guanylate cyclase activity in darkness. If Ca declines in light exponentially, $Ca(t) = Ca_0 \cdot \exp(-t/\tau)$, Eq. A22 yields

$$A(t) = \frac{A_{max}}{1 + (A_{max} - 1) \cdot \exp(-t \cdot n_{cyc}/\tau)}, \quad \text{(A23)}$$

which is essentially one of the terms in Eq. 2. If there are two independent regulations with magnitudes A_1 and A_2 and time constants τ_1 and τ_2, then the total regulation is given by the product of the two components (Eq. A19). Thus, we obtain Eq. 2. Note that the time constant obtained from the fit is n_{cyc} times faster than the time constant of Ca^{2+} decline.

This work was supported by the E. Mathilda Ziegler Foundation for the Blind, Inc. (to C.L. Makino), a Research to Prevent Blindness Career Development Award (to C.L. Makino), the US Civilian Research and Development Foundation RB1-217 (to V.I. Govardovskii and V.Y. Arshavsky), the Russian Foundation for Basic Research 01-04-49565 (V.I. Govardovskii) and the National Eye Institute awards Nos. EY12944 (to C.L. Makino), EY06857 (to P.D. Calvert), EY10336 (to V.Y. Arshavsky), and P30 EY12196 (to Harvard University).

Submitted: 16 October 2001
Revised: 10 December 2001
Accepted: 10 December 2001

REFERENCES

Arshavsky, V.Y., and M.D. Bownds. 1992. Regulation of deactivation of photoreceptor G protein by its target enzyme and cGMP. *Nature.* 357:416–417.

Arshavsky, V., M.P. Gray-Keller, and M.D. Bownds. 1991. cGMP suppresses GTPase activity of a portion of transducin equimolar to phosphodiesterase in frog rod outer segments. Light-induced cGMP decreases as a putative feedback mechanism of the photoresponse. *J. Biol. Chem.* 266:18530–18537.

Baylor, D.A., T.D. Lamb, and K.-W. Yau. 1979a. The membrane current of single rod outer segments. *J. Physiol.* 288:589–611.

Baylor, D.A., T.D. Lamb, and K.-W. Yau. 1979b. Responses of retinal rods to single photons. *J. Physiol.* 288:613–634.

Baylor, D.A., G. Matthews, and K.-W. Yau. 1980. Two components of electrical dark noise in toad retinal rod outer segments. *J. Physiol.* 309:591–621.

Baylor, D.A., B.J. Nunn, and J.L. Schnapf. 1984. The photocurrent, noise and spectral sensitivity of rods of the monkey *Macaca fascicularis*. *J. Physiol.* 357:575–607.

Blazynski, C., and A.I. Cohen. 1986. Rapid declines in cyclic GMP of rod outer segments of intact frog photoreceptors after illumination. *J. Biol. Chem.* 261:14142–14147.

Bondarenko, V.A., M. Desai, S. Dua, M. Yamazaki, R.H. Amin, K.K. Yousif, T. Kinumi, M. Ohashi, N. Komori, H. Matsumoto, et al. 1997. Residues within the polycationic region of cGMP phosphodiesterase γ subunit crucial for the interaction with transducin α subunit. Identification by endogenous ADP-ribosylation and site-directed mutagenesis. *J. Biol. Chem.* 272:15856–15864.

Bondarenko, V.A., M. Yamazaki, F. Hayashi, and A. Yamazaki. 1999. Suppression of GTP/Tα-dependent activation of cGMP phosphodiesterase by ADP-ribosylation by its γ subunit in amphibian rod photoreceptor membranes. *Biochemistry.* 38:7755–7763.

Bownds, D., A. Gordon-Walker, A.C. Gaide-Huguenin, and W. Robinson. 1971. Characterization and analysis of frog photoreceptor membranes. *J. Gen. Physiol.* 58:225–237.

Bownds, M.D., and V.Y. Arshavsky. 1995. What are the mechanisms of photoreceptor adaptation? *Behav. Brain Sci.* 18:415–424.

Burns, M.E., and D.A. Baylor. 2001. Activation, deactivation, and adaptation in vertebrate photoreceptor cells. *Annu. Rev. Neurosci.* 24:779–805.

Calvert, P.D., T.W. Ho, Y.M. LeFebvre, and V.Y. Arshavsky. 1998. Onset of feedback reactions underlying vertebrate rod photoreceptor light adaptation. *J. Gen. Physiol.* 111:39–51.

Cervetto, L., V. Torre, E. Pasino, P. Marroni, and M. Capovilla. 1981. Recovery from light-desensitization in toad rods. *In* Photoreceptors. A. Borsellino, and L. Cervetto, editors. Plenum Press, New York/London. 159–175.

Chen, C.-K., J. Inglese, R.J. Lefkowitz, and J.B. Hurley. 1995. Ca^{2+}-dependent interaction of recoverin with rhodopsin kinase. *J. Biol. Chem.* 270:18060–18066.

Cohen, A.I., and C. Blazynski. 1988. Light-induced losses and dark recovery rates of guanosine 3′,5′-cyclic monophosphate in rod outer segments of intact amphibian photoreceptors. *J. Gen. Physiol.* 92:731–746.

Cohen, A.I., and C. Blazynski. 1993. The determination of total cGMP levels in rod outer segments from intact toad photoreceptors in response to light superimposed on background and to consecutive flashes: a second light flash accelerates the dark recovery rate of cGMP levels in control media, but not in Na^+-free, low Ca^{2+} medium. *Vis. Neurosci.* 10:73–79.

Coles, J.A., and S. Yamane. 1975. Effects of adapting lights on the time course of the receptor potential of the anuran retinal rod. *J. Physiol.* 247:189–207.

Cote, R.H., M.D. Bownds, and V.Y. Arshavsky. 1994. cGMP binding sites on photoreceptor phosphodiesterase: role in feedback regulation of visual transduction. *Proc. Natl. Acad. Sci. USA.* 91:4845–4849.

Cote, R.H., and M.A. Brunnock. 1993. Intracellular cGMP concentration in rod photoreceptors is regulated by binding to high and moderate affinity cGMP binding sites. *J. Biol. Chem.* 268: 17190–17198.

Dawis, S.M., R.M. Graeff, R.A. Heyman, T.F. Walseth, and N.D. Goldberg. 1988. Regulation of cyclic GMP metabolism in toad photoreceptors. Definition of the metabolic events subserving photoexcited and attenuated states. *J. Biol. Chem.* 263:8771–8785.

de Azeredo, F.A.M., W.D. Lust, and J.V. Passonneau. 1981. Light-induced changes in energy metabolites, guanine nucleotides, and guanylate cyclase within frog retinal layers. *J. Biol. Chem.* 256: 2731–2735.

Dizhoor, A.M., E.V. Olshevskaya, W.J. Henzel, S.C. Wong, J.T. Stults, I. Ankoudinova, and J.B. Hurley. 1995. Cloning, sequencing, and expression of a 24-kDa Ca^{2+}-binding protein activating photoreceptor guanylyl cyclase. *J. Biol. Chem.* 270:25200–25206.

Dodd, R.L. 1998. The role of arrestin and recoverin in signal transduction by retinal rod photoreceptors: Ph.D. thesis. Stanford University, Palo Alto. 196 pp.

Donner, K., S. Hemila, G. Kalamkarov, A. Koskelainen, and T. Shevchenko. 1990. Rod phototransduction modulated by bicarbonate in the frog retina: roles of carbonic anhydrase and bicarbonate exchange. *J. Physiol.* 426:297–316.

Dowling, J.E., and H. Ripps. 1972. Adaptation in skate photoreceptors. *J. Gen. Physiol.* 60:698–719.

Fain, G.L. 1976. Sensitivity of toad rods: dependence on wavelength and background illumination. *J. Physiol.* 261:71–101.

Fain, G.L., T.D. Lamb, H.R. Matthews, and R.L.W. Murphy. 1989. Cytoplasmic calcium as the messenger for light adaptation in salamander rods. *J. Physiol.* 416:215–243.

Fain, G.L., H.R. Matthews, M.C. Cornwall, and Y. Koutalos. 2001. Adaptation in vertebrate photoreceptors. *Physiol. Rev.* 81:117–151.

Forti, S., A. Menini, G. Rispoli, and V. Torre. 1989. Kinetics of phototransduction in retinal rods of the newt *Triturus cristatus*. *J. Physiol.* 419:265–295.

Gordon, S.E., J. Downing-Park, and A.L. Zimmerman. 1995. Modulation of the cGMP-gated ion channel in frog rods by calmodulin and an endogenous inhibitory factor. *J. Physiol.* 486:533–546.

Govardovskii, V.I., and A.L. Berman. 1981. Light-induced changes of cyclic GMP content in frog retinal rod outer segments measured with rapid freezing and microdissection. *Biophys. Struc. Mech.* 7:125–130.

Govardovskii, V.I., N. Fyhrquist, T. Reuter, D.G. Kuzmin, and K. Donner. 2000. In search of the visual pigment template. *Vis. Neurosci.* 17:509–528.

Gray-Keller, M.P., and P.B. Detwiler. 1994. The calcium feedback signal in the phototransduction cascade of vertebrate rods. *Neuron.* 13:849–861.

Hare, W.A., and W.G. Owen. 1998. Effects of bicarbonate versus HEPES buffering on measured properties of neurons in the salamander retina. *Vis. Neurosci.* 15:263–271.

Hodgkin, A.L., and B.J. Nunn. 1988. Control of light-sensitive current in salamander rods. *J. Physiol.* 403:439–471.

Hsu, Y.-T., and R.S. Molday. 1993. Modulation of the cGMP-gated channel of rod photoreceptor cells by calmodulin. *Nature.* 361: 76–79.

Kawamura, S. 1993. Rhodopsin phosphorylation as a mechanism of cyclic GMP phosphodiesterase regulation by S-modulin. *Nature.* 362:855–857.

Klenchin, V.A., P.D. Calvert, and M.D. Bownds. 1995. Inhibition of rhodopsin kinase by recoverin. Further evidence for a negative feedback-system in phototransduction. *J. Biol. Chem.* 270:16147–16152.

Koch, K.-W., and L. Stryer. 1988. Highly cooperative feedback control of retinal rod guanylate cyclase by calcium ions. *Nature.* 334: 64–66.

Korschen, H.G., M. Beyermann, F. Muller, M. Heck, M. Vantler, K.-W. Koch, R. Kellner, U. Wolfrum, C. Bode, K.P. Hofmann, and U.B. Kaupp. 1999. Interaction of glutamic-acid-rich proteins with the cGMP signalling pathway in rod photoreceptors. *Nature.* 400: 761–766.

Koutalos, Y., K. Nakatani, T. Tamura, and K.-W. Yau. 1995a. Characterization of guanylate cyclase activity in single retinal rod outer segments. *J. Gen. Physiol.* 106:863–890.

Koutalos, Y., K. Nakatani, and K.-W. Yau. 1995b. The cGMP-phosphodiesterase and its contribution to sensitivity regulation in retinal rods. *J. Gen. Physiol.* 106:891–921.

Lagnado, L., and D.A. Baylor. 1994. Calcium controls light-triggered formation of catalytically active rhodopsin. *Nature.* 367:273–277.

Lagnado, L., L. Cervetto, and P.A. McNaughton. 1992. Calcium homeostasis in the outer segments of retinal rods from the tiger salamander. *J. Physiol.* 455:111–142.

Lagnado, L., and P.A. McNaughton. 1991. Net charge transport during sodium-dependent calcium extrusion in isolated salamander rod outer segments. *J. Gen. Physiol.* 98:479–495.

Lamb, T.D., and E.N. Pugh, Jr. 1992. A quantitative account of the activation steps involved in phototransduction in amphibian photoreceptors. *J. Physiol.* 449:719–758.

Leskov, I.B., V.A. Klenchin, J.W. Handy, G.G. Whitlock, V.I. Govardovskii, M.D. Bownds, T.D. Lamb, E.N. Pugh, Jr., and V.Y. Arshavsky. 2000. The gain of rod phototransduction: reconciliation of biochemical and electrophysiological measurements. *Neuron.* 27:525–537.

Lyubarsky, A., S. Nikonov, and E.N. Pugh, Jr. 1996. The kinetics of inactivation of the rod phototransduction cascade with constant Ca^{2+}_i. *J. Gen. Physiol.* 107:19–34.

Makino, C.L., L.N. Howard, and T.P. Williams. 1990. Axial gradients of rhodopsin in light-exposed retinal rods of the toad. *J. Gen. Physiol.* 96:1199–1220.

Matthews, H.R. 1990. Messengers of transduction and adaptation in vertebrate photoreceptors. *In* Light and Life in the Sea. P.J. Herring, A.K. Campbell, M. Whitfield, and L. Maddock, editors. Cambridge University Press, Cambridge. 185–198.

Matthews, H.R. 1996. Static and dynamic actions of cytoplasmic Ca^{2+} in the adaptation of responses to saturating flashes in salamander rods. *J. Physiol.* 490:1–15.

Matthews, H.R. 1997. Actions of Ca^{2+} on an early stage in phototransduction revealed by the dynamic fall in Ca^{2+} concentration during the bright flash response. *J. Gen. Physiol.* 109:141–146.

Matthews, H.R., M.C. Cornwall, and R.K. Crouch. 2001. Prolongation of actions of Ca^{2+} early in phototransduction by 9-demethylretinal. *J. Gen. Physiol.* 118:377–390.

Matthews, H.R., G.L. Fain, R.L.W. Murphy, and T.D. Lamb. 1990. Light adaptation in cone photoreceptors of the salamander: a role for cytoplasmic calcium. *J. Physiol.* 420:447–469.

Matthews, H.R., R.L.W. Murphy, G.L. Fain, and T.D. Lamb. 1988. Photoreceptor light adaptation is mediated by cytoplasmic calcium concentration. *Nature.* 334:67–69.

McCarthy, S.T., J.P. Younger, and W.G. Owen. 1996. Dynamic, spatially nonuniform calcium regulation in frog rods exposed to light. *J. Neurophysiol.* 76:1991–2004.

Meyertholen, E.P., M.J. Wilson, and S.E. Ostroy. 1986. The effects of HEPES, bicarbonate and calcium on the cGMP content of vertebrate rod photoreceptors and the isolated electrophysiological effects of cGMP and calcium. *Vision Res.* 26:521–533.

Murnick, J.G., and T.D. Lamb. 1996. Kinetics of desensitization induced by saturating flashes in toad and salamander rods. *J. Physiol.* 495:1–13.

Nakatani, K., Y. Koutalos, and K.-W. Yau. 1995. Ca^{2+} modulation of the cGMP-gated channel of bullfrog retinal rod photoreceptors. *J. Physiol.* 484:69–76.

Nakatani, K., and K.-W. Yau. 1988. Calcium and light adaptation in retinal rods and cones. *Nature.* 334:69–71.

Nikonov, S., N. Engheta, and E.N. Pugh, Jr. 1998. Kinetics of recovery of the dark-adapted salamander rod photoresponse. *J. Gen. Physiol.* 111:7–37.

Nikonov, S., T.D. Lamb, and E.N. Pugh, Jr. 2000. The role of steady phosphodiesterase activity in the kinetics and sensitivity of the light-adapted salamander rod photoresponse. *J. Gen. Physiol.* 116: 795–824.

Palczewski, K., I. Subbaraya, W.A. Gorczyca, B.S. Helekar, C.C. Ruiz, H. Ohguro, J. Huang, X. Zhao, J.W. Crabb, R.S. Johnson, et al. 1994. Molecular cloning and characterization of retinal photoreceptor guanylyl cyclase-activating protein. *Neuron.* 13:395–404.

Pepperberg, D.R., M.C. Cornwall, M. Kahlert, K.P. Hofmann, J. Jin, G.J. Jones, and H. Ripps. 1992. Light-dependent delay in the fall-

ing phase of the retinal rod photoresponse. *Vis. Neurosci.* 8:9–18.

Pepperberg, D.R., J. Jin, and G.J. Jones. 1994. Modulation of transduction gain in light adaptation of retinal rods. *Vis. Neurosci.* 11: 53–62.

Pugh, E.N., Jr., and T.D. Lamb. 2000. Phototransduction in vertebrate rods and cones: molecular mechanisms of amplification, recovery and light adaptation. *In* Handbook of Biological Physics: Molecular Mechanisms in Visual Transduction. vol. 3. D.G. Stavenga, W.J. DeGrip, and E.N. Pugh, Jr., editors. Elsevier Science, Amsterdam. 183–255.

Pugh, E.N., Jr., S. Nikonov, and T.D. Lamb. 1999. Molecular mechanisms of vertebrate photoreceptor light adaptation. *Curr. Opin. Neurobiol.* 9:410–418.

Reuter, T.E., R.H. White, and G. Wald. 1971. Rhodopsin and porphyropsin fields in the adult bullfrog retina. *J. Gen. Physiol.* 58:351–371.

Rieke, F., and D.A. Baylor. 1996. Molecular origin of continuous dark noise in rod photoreceptors. *Biophys. J.* 71:2553–2572.

Sagoo, M.S., and L. Lagnado. 1996. The action of cytoplasmic calcium on the cGMP-activated channel in salamander rod photoreceptors. *J. Physiol.* 497:309–319.

Tamura, T., K. Nakatani, and K.-W. Yau. 1991. Calcium feedback and sensitivity regulation in primate rods. *J. Gen. Physiol.* 98:95–130.

Tsuboi, S., H. Matsumoto, and A. Yamazaki. 1994. Phosphorylation of an inhibitory subunit of cGMP phosphodiesterase in *Rana catesbeiana* rod photoreceptors. II. A possible mechanism for the turnoff of cGMP phosphodiesterase without GTP hydrolysis. *J. Biol. Chem.* 269:15024–15029.

Xu, L.X., Y. Tanaka, V.A. Bonderenko, I. Matsuura, H. Matsumoto, A. Yamazaki, and F. Hayashi. 1998. Phosphorylation of the gamma subunit of the retinal photoreceptor cGMP phosphodiesterase by the cAMP-dependent protein kinase and its effect on the gamma subunit interaction with other proteins. *Biochemistry.* 37:6205–6213.

Yamazaki, A., V.A. Bondarenko, S. Dua, M. Yamazaki, J. Usukura, and F. Hayashi. 1996. Possible stimulation of retinal rod recovery to dark state by cGMP release from a cGMP phosphodiesterase noncatalytic site. *J. Biol. Chem.* 271:32495–32498.

Yau, K.-W., and K. Nakatani. 1984. Electrogenic Na-Ca exchange in retinal rod outer segment. *Nature.* 311:661–663.